Chinese Chemical Letters 32 (2021) 1953–1956

Contents lists available at ScienceDirect

Chinese Chemical Letters

journal homepage: www.elsevier.com/locate/cclet

Communication

Large scale synthesis of red emissive carbon dots powder by solid state reaction for fingerprint identification

Xiaoqing Niu, Tianbing Song, Huanming Xiong*

Department of Chemistry and Shanghai Key Laboratory of Molecular Catalysis and Innovative Materials, Fudan University, Shanghai 200438, China

ARTICLE INFO

Article history:
Received 5 December 2020
Received in revised form 31 December 2020
Accepted 4 January 2021
Available online 9 January 2021

Keywords:
Carbon dots
Red fluorescence
Solid reaction
Large scale
Fingerprint identification

ABSTRACT

Red emissive carbon dots (CDs) powder was synthesized on a large scale from phloroglucinol and boric acid by a novel solid state reaction with yield up to 75%. This method is safe and convenient, for it needs neither high pressure reactors nor complicated post-treatment procedures. The as-prepared carbon dots powder exhibited strong red fluorescence with excitation-independent behavior. XPS measurement and PL spectra suggest that such red fluorescence arise from boron-doped structures in CDs, which increases along with the boron concentration on CDs surface but decreases when the concentration quenching effect takes place. To overcome the aggregation induced fluorescence quenching of the solid CDs powder, the conventional methods are dispersing CDs into a large amount of inert substrates. But our present work provides a new strategy to realize strong red fluorescence of CDs in solid state. As a result, such carbon dots powder works well for latent fingerprint identification on various material surfaces.

Since fingerprint is regarded as the first evidence of trace physical evidence, much attention have been paid to the discovery, detection and extraction of fingerprints [1,2]. There are three types of fingerprints usually captured at crime scenes: visible fingerprints, indented fingerprints and latent fingerprints [3]. Among them, latent fingerprint is the most common problem in scene investigation, since it is difficult to distinguish and discover under normal circumstances. Therefore, latent fingerprint discovery and enhancement is crucial in order to make it serve for the investigation of cases and court proceedings. At present, traditional developing methods include powder dusting method, cyanoacrylate fuming method, silver nitrate method, ninhydrin method, 1,8-diazafluoren-9-one method and small particle reagent method [4–7]. Among them, the powder dusting method, which has been used in the late 19th century, is one of the oldest and popular methods for developing latent fingerprints on nonporous substrates [2,8]. Even so, its application is limited due to some difficulties, including low contrast, low sensitivity, low selectivity and high toxicity [8].

Recently, the application of fluorescent nanomaterials in the field of latent fingerprint identification has drawn extensive concerns on account of their peculiar optical properties to overcome the drawbacks of conventional methods. As a new generation of carbon-based fluorescent nanomaterials, carbon dots (CDs) are promising in the field of bioimaging and biosensing especially superiority in low toxicity [9–15]. And CDs are also naturally applied in the fingerprint identification [16–19]. First of all, the strong fluorescence signal of CDs can dramatically enhance the contrast and reduce background interference. Then, because the size of fluorescent nanomaterials is much smaller than the ridge details such as arches and terminations, using CDs to develop LFPs will have a high resolution [20]. In addition, CDs are almost non-toxic, which is important to the operators.

In the past decade, there has been an explosive development in synthetic methods of CDs, which can be classified as top-down and bottom-up strategies [21–28]. Although numerous raw materials have been explored to prepare CDs through the dehydration and condensation reaction, the harsh reaction conditions (*e.g.*, high temperature, high pressure, or strong acid) are usually required to synthesize CDs because the nucleation and growth of CDs heavily depend on these conditions [29]. Furthermore, CDs prepared from these routes usually have low yield that limits their wide applications. For development of LFPs, the most widely employed method is dusting LFPs with powder. However, CDs always suffer from the aggregation-induced quenching effects, so that their powder usually have no fluorescence. To overcome such a luminescence quenching effect, many inert substances have been used for CDs dispersion, such as $CaCO_3$ [30], sodium silicate [31], $BaSO_4$ [32] and SiO_2 [17]. We also employed starch to realize this function and obtained red emissive starch-CDs powder for dusting

* Corresponding author.
E-mail address: hmxiong@fudan.edu.cn (H. Xiong).

https://doi.org/10.1016/j.cclet.2021.01.006

LFP [19]. Obviously, the quality of the resulting LFPs images is highly dependent on the dispersion mediums which often induce light diffraction, low quantum yield and inhomogeneous luminescent intensity. Therefore, it is still a challenge to synthesize red emissive CDs powder without any dispersion mediums.

In this study, we present a rapid solid reaction to synthesize red emissive CDs powder directly in large scale. This reaction needs no solvent, no high pressure reactors and no post-treatment procedures. Without any dispersion mediums, the as-prepared CDs powder has a production yield up to 75% and a quantum yield up to 18.2%. They are employed as the fluorescent label for LFPs identification on different substrates, and the results confirm their strong red fluorescence is beneficial for LFPs imaging.

Experimentally, the CDs were synthesized by heating a solid mixture of phloroglucinol and boric acid in an open reactor at 200 °C for 3 h (Scheme 1). The molar ratio between phloroglucinol and boric acid was explored and the optimal ratio is 1:1 (Fig. S1 and Table S1 in Supporting information). Heating phloroglucinol solely without boric acid also produced some kind of nanoparticles which exhibit complicated emission spectra with multiple peaks from blue to red (Fig. S2 in Supporting information). Such nanoparticles are probably polymer dots because they cannot be observed clearly under HRTEM (Fig. S3 in Supporting information). In addition, the XRD patterns of the reaction products without or with boric acid in the reaction system were also collected. The results (Fig. S4 in Supporting information) show that there is no carbon dots signals for the sample free of boric acid, and only the original of phloroglucinol can be observed. But after boric acid is involved in the reaction, the products show diffraction peaks of carbon dots. With the increase of reaction time, the XRD peak tends to increase and narrow, indicating that carbon dots are growing larger gradually. Therefore, boric acid accelerates the formation of carbon dots, which plays the catalytic role in the reaction system. And thus, we think that in the present reaction, boric acid is not only a boron doping reagent, but also a catalyst to promote the dehydration and carbonization of phloroglucinol [26,27,33,34]. The CDs made from phloroglucinol and boric acid are uniform spherical nanoparticles with a mean size of 2.4 nm, and they have crystal graphite lattice with a typical (100) plane spacing of 0.21 nm (Fig. 1) [11]. Besides, the X-ray powder diffraction (XRD) pattern (Fig. S5 in Supporting information) shows a strong peak around 24°, corresponding to the typical (002) plane of graphite structure.

The structure of CDs was analyzed by Fourier transform infrared (FT-IR) spectra and X-ray photoelectron spectra (XPS). FT-IR spectra of CDs in Fig. 2a show two absorption band at 3293 cm^{-1} and 1346 cm^{-1}, corresponding to O—H and B—O stretching vibrations respectively [35]. The characteristic stretching vibrations of C=C are observed at 1400-1600 cm^{-1}. The band at about 1156 cm^{-1} is attributed to the asymmetrically stretching oxygen atoms connected to the trigonal boron atoms [36]. These

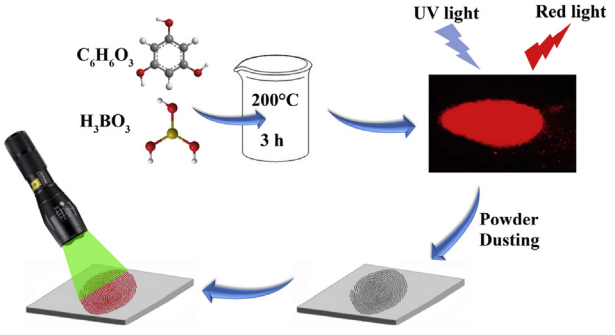

Scheme 1. Synthesis of red emissive CDs powder for dusting and imaging LFPs.

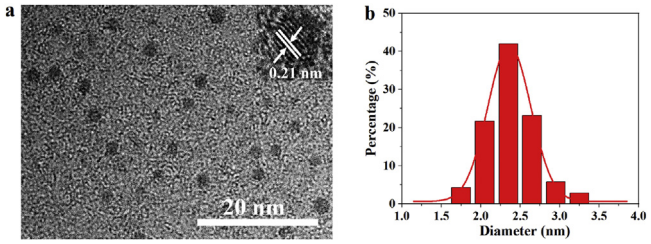

Fig. 1. (a) TEM image and the inset HRTEM image of CDs. (b) Size distribution of CDs.

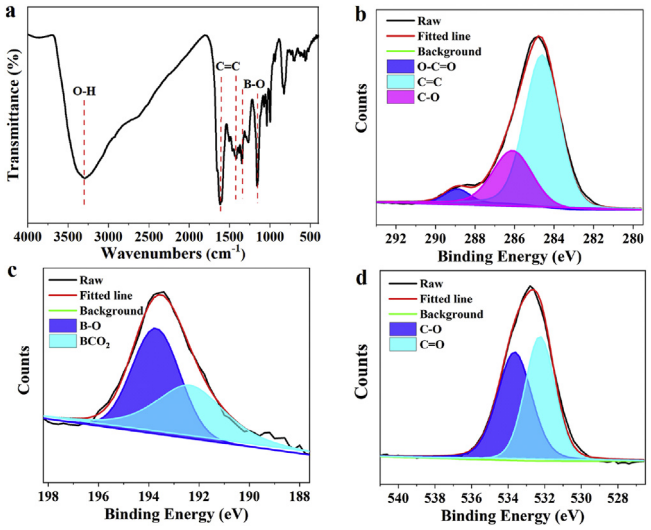

Fig. 2. (a) FT-IR spectrum of CDs. High resolution XPS analyses of (b) C 1s, (c) B 1s and (d) O 1s of CDs, respectively.

results are in agreement with XPS analyses. In Fig. S6 (Supporting information), the survey spectrum of XPS confirm that CDs are composed of C (72.56%), O (25.23%) and B (2.21%) elements, indicating boron has doped into CDs successfully. The high resolution spectrum of C 1s (Fig. 2b) reveal the presence of O—C=O, C=C and C—O functional groups. The B 1s spectrum (Fig. 2c) was deconvoluted into two peaks, representing B—O and BCO_2 respectively. The O 1s spectrum (Fig. 2d) also involves two peaks, which are attributed to C—O and C=O respectively.

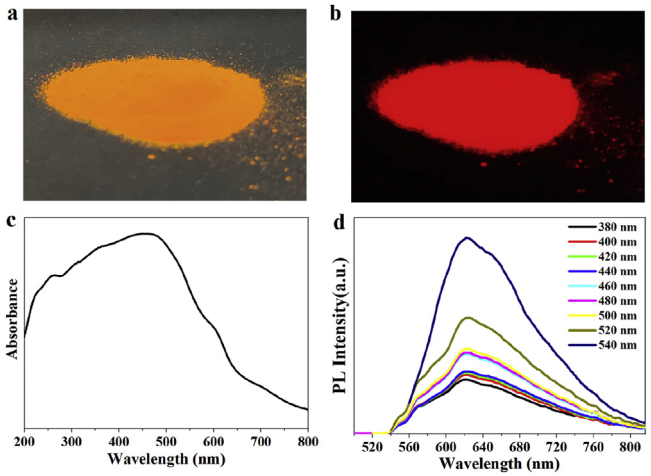

Fig. 3. CDs powder under (a) day light and (b) UV lamp, respectively. (c) Absorption spectrum and (d) PL spectra of CDs powder.

The CDs powder looks orange in the room light (Fig. 3a), but emits red fluorescence under UV light (Fig. 3b). The UV–vis absorption curve in Fig. 3 shows such CDs powder has a wide range of absorption, indicating a wide wavelength range of light can make the powder luminescent. The absorption peak around 260 nm was attributed to π-π^* transitions of sp^2 π-conjugation domains of CDs, while the lower energy absorption bands at around 460 nm are typically connected with narrowing of the electronic band gap which is often observed in red fluorescent CDs [37,38]. The photoluminescent (PL) emission spectra in Fig. 3d confirm the above features of our CDs and show the strongest emission intensity when the excitation light wavelength is 540 nm. And thus, green light is employed for the LFPs imaging.

It is obvious that our CDs' PL emission spectra exhibit the typical excitation independent behavior, *i.e.*, the PL emission band do not shift when the wavelength of excitation light changes. This phenomenon indicates both composition and structure of our CDs are uniform, and the corresponding luminescent centers are uniform, too. Since the boron doing is crucial to the solid state luminescence in this research, CDs doped with different amounts of boron element were synthesized and their luminescent spectra and quantum yields were measured, respectively. Table S1 shows that when boron content increases from 0.39 wt% to 4.71 wt% (measured by XPS in Fig. S7 in Supporting information), the PLQY of the corresponding CDs increases from 5.63% to 18.2%. But more boron doping induces luminescence decay. For all samples, the PL emission centers at about 620 nm, which is beneficial for LFPs imaging.

The photoluminescent mechanisms of CDs remain controversial at present, because there are many types of CDs and each type of CDs have various and complicated structures. Most of CDs lose their fluorescence in solid state due to the typical aggregation induced quenching effect. But for our CDs, the solid state fluorescence highly depends on the doped B concentration, indicating a special luminescent mechanism. According to the above spectra analyses, we believe that the red fluorescence arises from the doped boron species with the surrounding carbon structures. When the B doping content is low, these luminescent centers are dispersed and diluted, so their emission processes will not interfere with each other. But when the B concentration is too high, the concentration quenching effect will take place and the whole fluorescence will decay. A possible luminescent mechanism is suggested in Scheme 2, in which Boron containing emission centers are responsible for the red fluorescence.

Owing to their strong solid state red fluorescence, such CDs are good phosphor powder for dusting LFPs on different substrates. After development on a glass sheet, the LFPs image can be seen clearly under a green laser irradiation. All details of the LFPs are identified, including terminations, crossovers, islands, bifurcations, cores and scars (Fig. 4). For comparison, the same fingerprint is also pressed on a metal foil and a plastic sheet (Fig. S8 in Supporting information), respectively, followed by the same development. It is clear that the details of such LFPs on different substrate are consistent, confirming that the dusting method by our CDs is reliable and reproducible. The photostability of CDs powder was determined with strong UV lamp under continuous irradiation. The results (Fig. S9a in Supporting information) show that the fluorescence intensity of CDs powder does not decay significantly under UV light irradiation for 1 h. Besides, we also provide the fluorescence spectra of CDs powder (Fig. S9b in Supporting information) after a long term storage in the air to show the fluorescence stability of CDs powder. In addition, the LFPs developed by our CDs keep stable after 30 days storage without any protection (Fig. S10 in Supporting information), which ensures the practical applications of this method.

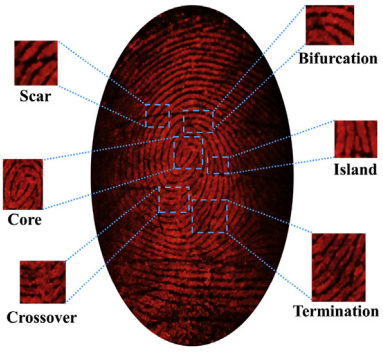

Fig. 4. A fluorescence image of LFPs on a glass sheet developed by a powder dusting method with CDs powder under green light irradiation, along with the magnified images of the feature details.

In summary, we invented a convenient, efficient, green and safe method to synthesize fluorescent CDs powder *via* a simple solid state reaction with a high product yield. The obtained CDs are monodispersed and uniform spherical nanoparticles with abundant functional groups, especially the boron-containing groups. The CDs powder shows strong red emission under a wide wavelength range of irradiation light. Such a solid state fluorescence, free of the classical aggregation-induced quenching effect, is ascribed to the doped boron species with the surrounding carbon structures. Based on such a novel mechanism and a special structure, our CDs exhibited a long-term stable fluorescence with considerable PLQY. When they were applied for LFPs identification by the powder dusting method, the resulting images showed detailed features with high contrast, high sensitivity and low background interference. Therefore, our present work provides a new strategy for mass production of fluorescent CDs powder, which has a promising application for LFPs identification.

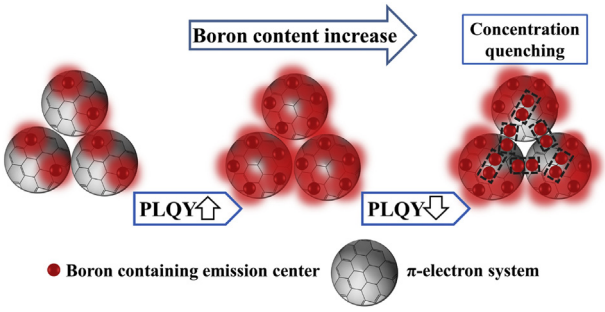

Scheme 2. A possible solid-state fluorescence mechanism for B-doped CDs.

Declaration of competing interest

The authors report no declarations of interest.

Acknowledgments

This work was financially supported by the National Natural Science Foundation of China (Nos. 21975048, 21771039), and the Science and Technology Commission of Shanghai Municipality (No. 19DZ2270100).

Appendix A. Supplementary data

Supplementary material related to this article can be found, in the online version, at doi:https://doi.org/10.1016/j.cclet.2021.01.006.

References

[1] P. Hazarika, D.A. Russell, Angew. Chem. Int. Ed. 51 (2012) 3524–3531.
[2] H. Faulds, Nature 22 (1880) 605.
[3] H.C. Lee, R.E. Gaensslen, Advances in Fingerprint Technology, 2nd ed., CRC Press, Boca Raton, 2001.
[4] Z. Qiu, B. Hao, X. Gu, et al., Sci. China Chem. 61 (2018) 966–970.
[5] H. Chen, R.L. Ma, Z. Fan, et al., J. Colloid Interface Sci. 528 (2018) 200–207.
[6] F.M. Kerr, A.D. Westland, F. Haque, Forensic Sci. Int. 18 (1981) 209–214.
[7] L. Schwarz, I. Klenke, J. Forensic Sci. 52 (2007) 649–655.
[8] M. Wang, M. Li, A. Yu, et al., Adv. Funct. Mater. 27 (2017) 1606243.
[9] H. Li, Z. Kang, Y. Liu, et al., J. Mater. Chem. 22 (2012) 24230–24253.
[10] S. Ruan, J. Qian, S. Shen, et al., Nanoscale 6 (2014) 10040–10047.
[11] H. Ding, S.B. Yu, J.S. Wei, et al., ACS Nano 10 (2016) 484–491.
[12] J. Zhong, X. Chen, M. Zhang, et al., Chin. Chem. Lett. 31 (2020) 769–773.
[13] C. Liu, L. Bao, B. Tang, et al., Small 12 (2016) 4702–4706.
[14] H. Wang, J. Wei, C. Zhang, et al., Chin. Chem. Lett. 31 (2020) 759–763.
[15] S. Lu, L. Sui, J. Liu, et al., Adv. Mater. 29 (2017) 1603443.
[16] J. Chen, J.S. Wei, P. Zhang, et al., ACS Appl. Mater. Interfaces 9 (2017) 18429–18433.
[17] D. Peng, X. Liu, M. Huang, et al., Dalton Trans. 47 (2018) 5823–5830.
[18] C. Wang, J. Zhou, L. Lulu, et al., Part. Part. Syst. Charact. 35 (2018) 1700387.
[19] X.Y. Dong, X.Q. Niu, Z.Y. Zhang, et al., ACS Appl. Mater. Interfaces 12 (2020) 29549–29555.
[20] M. Wang, M. Li, A. Yu, et al., ACS Appl. Mater. Interfaces 7 (2015) 28110–28115.
[21] K. Hola, Y. Zhang, Y. Wang, et al., Nano Today 9 (2014) 590–603.
[22] M. Han, S. Zhu, S. Lu, et al., Nano Today 19 (2018) 201–218.
[23] X. Tan, Y. Li, X. Li, et al., Chem. Commun. (Camb.) 51 (2015) 2544–2546.
[24] J. Liu, D. Li, K. Zhang, et al., Small 14 (2018) 1703919.
[25] W. Li, Y. Liu, B. Wang, et al., Chin. Chem. Lett. 30 (2019) 2323–2327.
[26] H. Ding, J.S. Wei, P. Zhang, et al., Small 14 (2018) 1800612.
[27] F. Yuan, T. Yuan, L. Sui, et al., Nat. Commun. 9 (2018) 2249.
[28] B. Wang, J. Li, Z. Tang, et al., Sci. Bull. (Beijing) 64 (2019) 1285–1292.
[29] B. Yao, H. Huang, Y. Liu, et al., Trends Analyt. Chem. 1 (2019) 235–246.
[30] S. Guo, M. Yang, M. Chen, et al., Dalton Trans. 44 (2015) 8232–8237.
[31] Z. Tian, X. Zhang, D. Li, et al., Adv. Optical Mater. 5 (2017) 1700416.
[32] D. Zhou, Y. Zhai, S. Qu, et al., Small 13 (2017) 1602055.
[33] K. Jiang, Y. Wang, X. Gao, et al., Angew. Chem. Int. Ed. 57 (2018) 6216–6220.
[34] H. Song, X. Liu, B. Wang, et al., Sci. Bull. (Beijing) 64 (2019) 1788–1794.
[35] W. Lei, D. Portehault, R. Dimova, et al., J. Am. Chem. Soc. 133 (2011) 7121–7127.
[36] W. Li, W. Zhou, Z. Zhou, et al., Angew. Chem. Int. Ed. 58 (2019) 7278–7283.
[37] K. Jiang, S. Sun, L. Zhang, et al., Angew. Chem. Int. Ed. 54 (2015) 5360–5363.
[38] M. Vázquez-González, W.C. Liao, R. Cazelles, et al., ACS Nano 11 (2017) 3247–3253.